Modes and Attenuation Constants in Circular Hollow Waveguides with Small Core Diameters for the Infrared

Yuji Kato and Mitsunobu Miyagi, *Senior Member, IEEE*

Abstract—**The mode structures and attenuation constants in circular hollow waveguides are evaluated numerically based on the exact characteristic equations. Mode properties, which are strongly dependent on waveguide materials, and attenuation constants are discussed when the core diameter becomes small. Special modes are also analyzed in oversized metallic waveguides which approach very familiar modes in perfect-conducting cylindrical waveguides when the core diameter becomes small.**

I. Introduction

HOLLOW waveguides are promising media for transmitting high-powered infrared laser light as emitted by carbon dioxide (CO_2) and carbon monoxide (CO) lasers. Many kinds of hollow waveguides have been proposed [1]–[6]. In particular, dielectric-coated metallic hollow waveguides have been shown to have low losses when the metals and the dielectric coatings are suitably chosen [6], [7]. Transmission of 1 kW CO_2 laser light has been achieved with losses of 0.05 dB/m by germanium-coated silver waveguides with a core diameter of 1.5 mm [8]. For some medical uses, there is a need for smaller core waveguides with moderate power capability in recent [9]. So far, the attenuation constants in hollow waveguides are estimated based on the approximate characteristic equation by assuming that the core diameters are sufficiently large [6], [10]. But the attenuation constants as well as the mode structure should be examined more precisely when the cores of waveguides become small.

In this paper, we present numerical results of the exact characteristic equations to determine the attenuation constants of the modes in hollow waveguides with arbitrary core diameters. Relations between modes in small and large core waveguides have been made clear completely and electric field lines have been also presented to show the relations clearly. In hollow waveguides such as sapphire and silica waveguides whose absolute value of the complex refractive index is small, the HE_{11} mode maintains its property even when the core diameter becomes very small, which is very different from that in ordinary metallic waveguides. Special modes in large core metallic hollow waveguides are also analyzed which approach very familiar modes in perfect-conducting cylindrical waveguides.

Manuscript received December 12, 1990; revised November 7, 1991. This work was supported by a Scientific Research Grant-in-Aid (02402036) from the Ministry of Education, Science and Culture of Japan.

The authors are with the Department of Electrical Communications, Faculty of Engineering, Tohoku University, Sendai, 980 Japan.

IEEE Log Number 9106047.

II. Characteristic Equations of the Modes in Hollow Waveguides

Consider a waveguide consisting of a cylinder of radius T and refractive index $n_0(\simeq 1)$ embedded in a medium with a refractive index $n_0 n_1$. The z-components of electric field E_z and magnetic field H_z are expressed in the cylindrical coordinate (r, θ, z) as follows [11]:

$$E_z = \begin{cases} J_n\left(u_0 \dfrac{r}{T}\right) \cos(n\theta + \theta_0) & (r < T) \\ \dfrac{J_n(u_0)}{H_n^{(2)}(u_1)} H_n^{(2)}\left(u_1 \dfrac{r}{T}\right) \cos(n\theta + \theta_0) & (r > T) \end{cases} \tag{1}$$

$$H_z = \begin{cases} -\dfrac{\beta}{\omega\mu_0} P J_n\left(u_0 \dfrac{r}{T}\right) \sin(n\theta + \theta_0) & (r < T) \\ -\dfrac{\beta}{\omega\mu_0} P \dfrac{J_n(u_0)}{H_n^{(2)}(u_1)} H_n^{(2)}\left(u_1 \dfrac{r}{T}\right) \cdot \sin(n\theta + \theta_0) & (r > T) \end{cases} \tag{2}$$

where the normalized transverse phase constants in the core and cladding are u_0 and u_1, respectively. They are related to the axial complex phase constant $\beta\ (= \beta_0 - j\alpha)$ as

$$\beta^2 + \left(\frac{u_0}{T}\right)^2 = (n_0 k_0)^2, \tag{3}$$

$$\beta^2 + \left(\frac{u_1}{T}\right)^2 = (n_0 n_1 k_0)^2, \tag{4}$$

where k_0 is a wavenumber of the plane wave in a free space, and P is an arbitrary constant to be determined.

By using the boundary condition that the tangential electric and magnetic fields are continuous at $r = T$, one obtains

$$(\eta_0 - \eta_1)(\eta_0 - n_1^2\eta_1) = n^2\left(\frac{1}{u_0^2} - \frac{1}{u_1^2}\right)\left(\frac{1}{u_0^2} - \frac{n_1^2}{u_1^2}\right), \tag{5}$$

where η_0 and η_1 are defined by

$$\eta_0 = \frac{J_n'(u_0)}{u_0 J_n(u_0)}, \tag{6}$$

$$\eta_1 = \frac{H_n^{(2)\prime}(u_1)}{u_1 H_n^{(2)}(u_1)}. \tag{7}$$

By eliminating β from (3) and (4), one obtains

$$u_1^2 - u_0^2 = (n_1^2 - 1)(n_0 k_0 T)^2. \tag{8}$$

Equations (5) and (8) are exact characteristic equations describing mode properties in hollow waveguides with arbitrary core diameters. By solving the equations, the axial phase constant β_0 and the attenuation constant α are obtained from (3). On the other hand, the parameter P in (2), which is used for mode designation [12]–[14], is expressed by

$$P = n\left(\frac{1}{u_0^2} - \frac{1}{u_1^2}\right)\Big/(\eta_0 - \eta_1). \tag{9}$$

We employ the Müller's method [15] to seek a complex solution u_0 of the characteristic equations (5) and (8), and use the asymptotic expansion formula [16] for the second kind Hankel function $H_n^{(2)}(u_1)$.

Throughout the paper, the wavelength is assumed to be 10.6 μm of the CO_2 laser light.

III. Metallic Hollow Waveguide

We first clearify the mode properties in metallic waveguides. We numerically evaluate the attenuation constants and P values of the modes in the hollow waveguides as functions of the core diameter. Next, we compare attenuation constants numerically obtained with those by the approximate analytical method [6].

A. Mode Structure

We consider a nickel (Ni) hollow waveguide, whose complex refractive index is 7.39–j39.3 [17], as a metallic hollow waveguide. We discuss relations between modes in the small and large core waveguides.

Fig. 1 shows P_N defined by

$$P_N = |P|^2/(1 + |P|^2), \tag{10}$$

for the hybrid HE_{11} and EH_{11} modes. In the large core waveguide, P_N is nearly equal to 0.5 for the hybrid modes, because P is nearly equal to -1 for the HE_{11} mode and 1 for the EH_{11} mode. When the core diameter becomes small, $|P|$ approaches 0 or infinity, which means that the HE_{11} mode approaches the TM mode without H_z and the EH_{11} mode goes to the TE mode without E_z. This means that mode properties change completely with the core diameter.

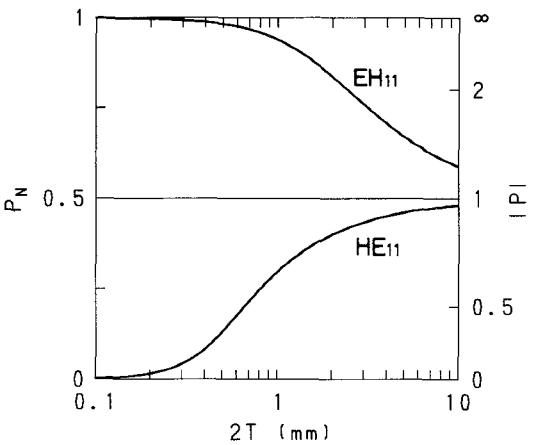

Fig. 1. P_N of the HE_{11} and EH_{11} modes in a Ni hollow waveguide as functions of core diameter.

In order to see what modes the HE_{11} and EH_{11} modes approach and also to see properties of other lower order modes, we show real and imaginary parts of the normalized transverse phase constants u_0 as functions of the core diameter in Fig. 2(a) and (b). There are crossing points in Re (u_0) and Im (u_0) of some modes. However, they occur at the different core diameters. Therefore, no mode degeneration occurs. Re (u_0) of the HE_{11} mode varies from j_{01} (= 2.4048) to j_{11} (= 3.8317) and that of the EH_{11} mode varies from j_{21} (= 5.1356) to j_{12}' (= 5.3314) when the core diameter decreases. We first point out that the HE_{11} and EH_{11} modes in the large core waveguide gradually approach the TM_{11} and TE_{12} modes in the small core waveguide, respectively. These mode changes or transitions are clearly understood by electric field lines of the modes as shown in Fig. 3(a) and (b). These field lines are obtained by solving a differential equation:

$$\frac{dr}{r\,d\theta} = \frac{E_r}{E_\theta}, \tag{11}$$

where we have neglected Im (u_0) because it is much smaller than Re (u_0) and also neglected the imaginary part of P reasonably. One should note that the TM_{11} and TE_{12} modes in the small core waveguide, e.g., $2T$ = 0.1 mm, are almost the same with those in a perfect-conducting cylindrical waveguide. It is also noted that the TM_{01} mode in the large core waveguide approaches the TM_{02} mode in the small core waveguide because Re (u_0) of the TM_{01} mode varies from j_{11} (= 3.8317) to j_{02} (= 5.5201). On the other hand, the TE_{01} mode does not change at all because Re (u_0) of the TE_{01} mode changes little.

There exist the TM_{01} and TE_{11} modes in the small core waveguide [6]. However, as is shown in Fig. 2(a) and (b), Re $(u_0)'$ as well as Im $(u_0)'$ of these two modes increase when the core diameter becomes large. These modes do not correspond to the well-known modes, e.g., TE, TM, HE, or EH mode, in the large core waveguide whose properties have not ever been analyzed in detail [18]. Therefore, we tentatively call these two modes in the large core waveguide TM_0' and TM_1' modes, respectively. For the TE_{11} mode, $|P|$ becomes very small with increasing

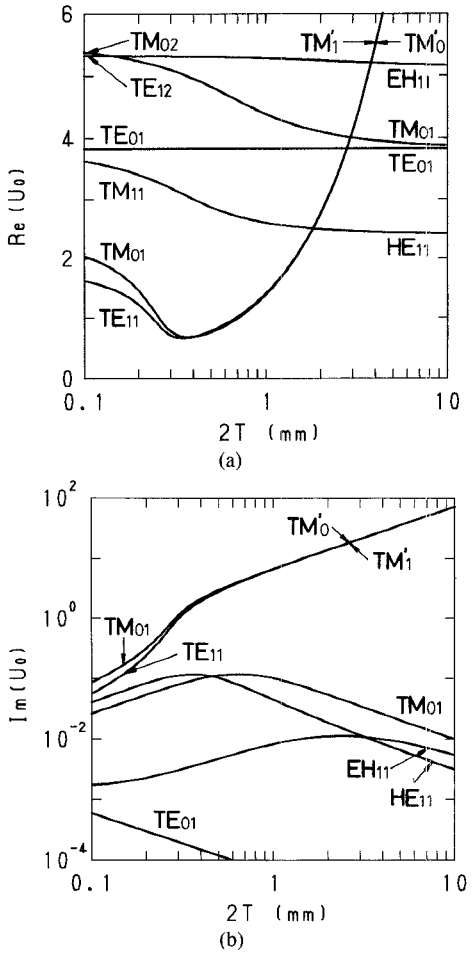

Fig. 2. u_0 of the HE_{11}, EH_{11}, TM_{01}, and TE_{01} modes in a large core Ni hollow waveguide and those of TE_{11} and TM_{01} modes in a small core one as functions of core diameter. (a) Real part of u_0. (b) Imaginary part of u_0.

core diameter and the mode approaches a TM mode without H_z. To see how the TE_{11} mode approaches the TM_1' mode, we show the variation of electric field lines in Fig. 4. As Im (u_0) and Im (P) of the TM_1' and TM_0' modes cannot be neglected in the large core waveguides, the electric field at each position in a hollow core region is elliptically polarized with different degrees of polarization. As we have numerically proved that the degree of polarization is greater than 0.9, we draw the electric field lines as the solution of

$$\frac{dr}{r\,d\theta} = \frac{|E_r|}{|E_\theta|}. \tag{12}$$

The electric field lines of the TE_{11} mode resemble those of the TM_{0m} mode, which are radial from the center of the core, when the core diameter becomes large. Distributions of $|E_r|$ of the TE_{11} and TM_{01} modes whose nomenclature is given in the small core waveguide are shown in Figs. 5 and 6 at $\theta = 0$ as functions of the core diameter. It can be seen that the field distributions of both modes in the large core waveguides are very similar each other, which corresponds to the resemblance of dispersion curves in Fig. 2(a) and (b). One should note that field distributions of the TM_{01} denoted by dashed lines and TM_0' modes are completely different as is seen from Fig. 6.

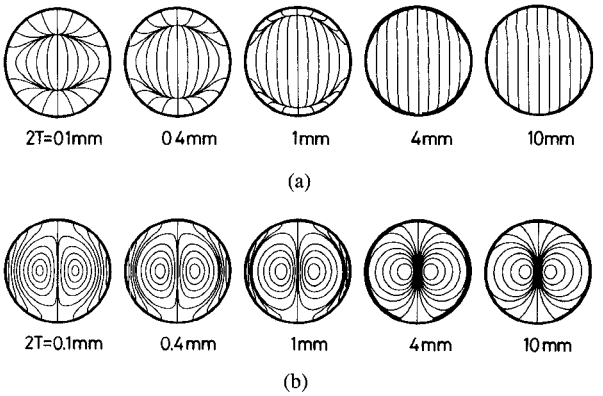

Fig. 3. Electric field lines of the HE_{11} and EH_{11} modes in a large core Ni hollow waveguide which approach the TM_{11} and TE_{12} modes in a small core hollow waveguides. (a) HE_{11} mode. (b) EH_{11} mode.

Gastine *et al.* [19] investigated "exterior" modes in free dielectric spheres and pointed out that the real and imaginary parts of characteristic equation solutions of those modes, which correspond to the transverse phase constants, tend toward infinity with increasing dielectric constants of the spheres. The TM_0' and TM_1' modes which we have found in a metallic cylindrical waveguide are similar to the "exterior" modes, although Gastine *et al.*, didn't show field distributions in a whole region. However, considering that the refractive index of core region is not large in our waveguide and also the modes have the perpendicular polarization to the metallic wall, it might be reasonable to call them plasmon [20], [21] in the cylindrical structure.

Re $(u_0)'$ of other higher order HE_{1m}, EH_{1m}, TE_{0m}, and TM_{0m} $(m = 2, 3, \cdots, 5)$ modes are numerically evaluated and the relation of modes in small and large core waveguides as well as F factor in (13) are summarized in Table I.

B. Attenuation Constant

Fig. 7 shows power attenuations of the HE_{11}, EH_{11}, TE_{01}, and TM_{01} modes. When the core diameter is large, attenuation of these modes are inversely proportional to the cube of the core diameter as is expected. However, increments of attenuation constants become small as the core diameter becomes small. It should be noted that the attenuation of the EH_{11} mode which approaches the TE_{12} mode becomes lower than that of the HE_{11} mode approaching the TM_{11} mode as the core diameter becomes small.

The attenuation of the TE_{01} mode is inversely proportional to the cube of core diameter in the region of the core diameter down to 0.1 mm. However, the attenuation of the TM_{01} mode is inversely proportional to the core diameter rather than to the cube as the core diameter becomes small.

Now, we compare the attenuation constants obtained numerically and those predicted by the previous theory [6]. By using a normalized surface impedance z_{TE} and ad-

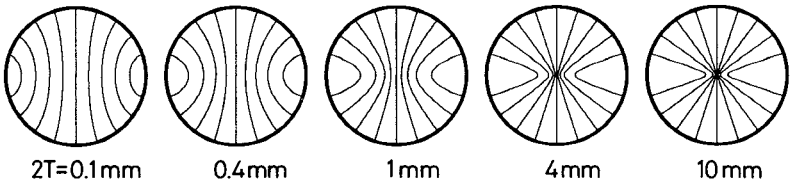

Fig. 4. Electric field lines of the TE_{11} mode whose nomenclature is given in a small core Ni hollow waveguide with various core diameters.

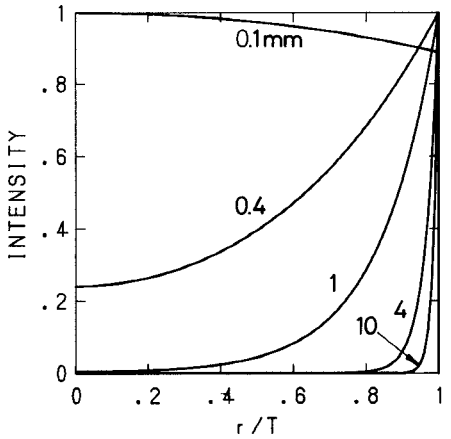

Fig. 5. Electric field intensity distributions of the TE_{11} mode in a small core Ni hollow waveguide with various core diameters.

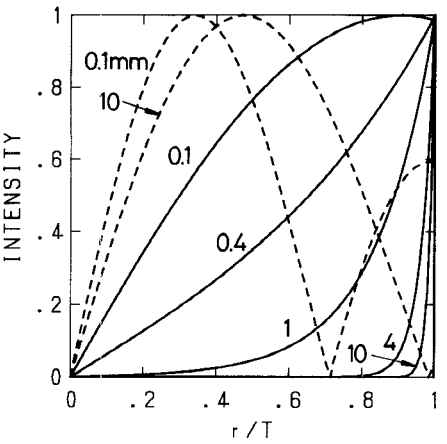

Fig. 6. Electric field intensity distributions of the TM_{01} and TM_{02} modes in a small core Ni hollow waveguide with various core diameters. The solid and dashed lines correspond to the TM_{01} and TM_{02} modes whose nomenclature is given in a small core waveguide, respectively.

TABLE I
MODE TRANSITIONS AND APPROXIMATE ATTENUATION CONSTANTS IN THE Ni HOLLOW WAVEGUIDE, WHERE j_{nm} AND j'_{nm} REPRESENT THE mth ZERO POINTS OF $J_n(u_0)$ AND $J'_n(u_0)$ EXCEPT FOR ZERO, RESPECTIVELY

$n_0k_0T \gg \lvert z_{TE}\rvert$ and $n_0k_0T \gg \lvert y_{TM}\rvert$				$n_0k_0T \gg \lvert z_{TE}\rvert$ and $n_0k_0T \ll \lvert y_{TM}\rvert$		
Mode	F	Re (u_0)		Mode	F	Re (u_0)
TE_{0m}	(a) Re (z_{TE})	j_{1m}	→	TE_{0m}	(a) Re (z_{TE})	j_{1m}
EH_{1m}	(d) $\frac{1}{2}$ Re $(z_{TE} + y_{TM})$	j_{2m}	→	TE_{1m+1}	(b) $\frac{1}{1-(1/u_0)^2} \cdot$ Re $\left[z_{TE} + \frac{1}{u_0^4}\frac{(n_0k_0T)^2}{y_{TM}}\right]$	j'_{1m+1}
HE_{1m}		j_{0m}	→	TM_{1m}	(c) $\left(\frac{n_0k_0T}{u_0}\right)^2$ Re $\left(\frac{1}{y_{TM}}\right)$	j_{1m}
TM_{0m}	(e) Re (y_{TM})	j_{1m}	→	TM_{0m+1}		j_{0m+1}

mittance y_{TM}, the theory predicts the attenuation constant α as

$$\alpha = n_0k_0 \frac{u_0^2}{(n_0k_0T)^3} F, \tag{13}$$

where the factor F is summarized in Table I for the two extreme cases of core diameters. In the case of hollow waveguides consisting of a single cladding with a refractive index of n_0n_1, z_{TE} and y_{TM} become

$$z_{TE} = \frac{1}{\sqrt{n_1^2 - 1}}, \tag{14}$$

$$y_{TM} = \frac{n_1^2}{\sqrt{n_1^2 - 1}}. \tag{15}$$

Attenuations estimated by (13) are shown in Fig. 7 for comparison. Each dotted line indicates the approximate attenuation in the Ni hollow waveguide either when the core diameter is large ($|z_{TE}| \ll n_0k_0T$, $|y_{TM}| \ll n_0k_0T$) or small ($|z_{TE}| \ll n_0k_0T$, $|y_{TM}| \gg n_0k_0T$). As is seen in Fig. 7, the attenuations of these modes are evaluated precisely by (13) when the approximate attenuation formulas are suitably used. However, there are wide ranges of core diameters where (13) cannot predict proper losses of modes except for the TE_{01} mode.

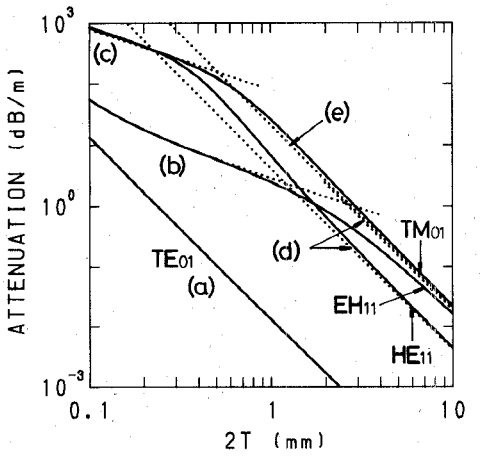

Fig. 7. Attenuation constants of the HE_{11}, EH_{11}, TM_{01}, and TE_{01} modes in a Ni hollow waveguide as functions of core diameter. The solid and dotted lines correspond to the numerical results and approximate ones obtained by using (13) with (a)–(e) in Table I, respectively.

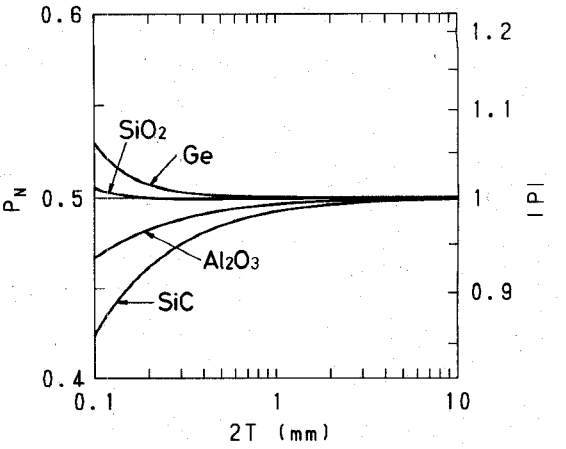

Fig. 8. P_N of the HE_{11} mode in various dielectric hollow waveguides as functions of core diameter, where $n - j\kappa$ is equal to 0.67–j0.03 (Al_2O_3) [5], 2.22–j0.1 (SiO_2) [17], 0.059–j1.21 (SiC) [17], and 4–j0 (Ge) [17], respectively.

IV. Dielectric Hollow Waveguides

We consider several kinds of hollow waveguides consisting of dielectric materials whose imaginary parts κ of complex refractive indices are relatively small.

In Fig. 8, P_N of the HE_{11} mode in the large core waveguides are shown as functions of core diameter. The HE_{11} mode in sapphire (Al_2O_3), silicon carbide (SiC), and silica (SiO_2) waveguides is likely to approach the TM mode, whereas the HE_{11} mode in a germanium (Ge) hollow waveguide to the TE mode. However, drastic changes of mode properties are not found as observed in the Ni hollow waveguide. In particular, the HE_{11} mode in the SiO_2 waveguide preserves its property even when the core diameter becomes very small down to 0.1 mm.

Fig. 9 shows power attenuation of the HE_{11} mode in those hollow waveguides. It is seen that the numerical and approximate attenuations predicted by (13) are in good agreement in the hollow waveguides.

For the higher hybrid HE_{1m} and EH_{1m} (m = 2, 3, $\cdots$, 5) modes, numerical calculations have been conducted to see how the mode property changes and the results are summarized in Table II for the modes in dielectric as well as metallic waveguides.

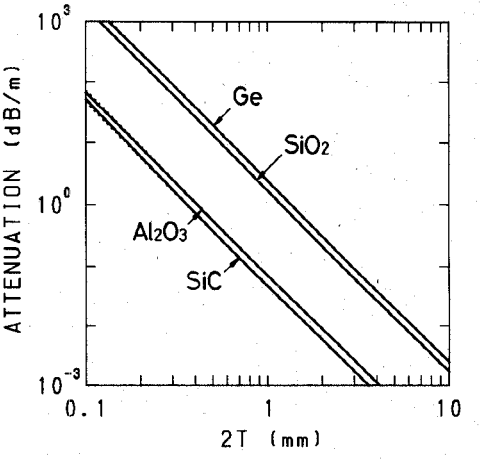

Fig. 9. Attenuation constants of the HE_{11} mode in various dielectric hollow waveguides as functions of core diameter. The solid and dotted lines correspond to the numerical attenuations and those obtained by using (13) which are inversely proportional to the cube of core diameter.

TABLE II
Mode Transitions in Various Hollow Waveguides

Core Diameter		
Large		Small
HE_{1m}		TE
EH_{1m}		TM

The solid lines correspond to the HE_{1m} and EH_{1m} (m = 1, $\cdots$, 5) modes in Ni, Al_2O_3, and SiC hollow waveguides, and the HE_{1m} (m = 3, $\cdots$, 5) and EH_{1m} (m = 2, $\cdots$, 5) in a SiO_2 hollow waveguide. The dashed lines correspond to the HE_{1m} and EH_{1m} (m = 1, $\cdots$, 5) modes in a Ge hollow waveguide and the HE_{1m} (m = 1, 2) and EH_{11} in a SiO_2 hollow waveguide.

V. Material Dependent Mode Transitions

As mentioned above, mode properties strongly depend on cladding materials, mode orders, and core diameters of the hollow waveguides. We focus our attention to the HE_{11} mode and estimate the regions in the plane of complex refractive index ($n - j\kappa$) of cladding material where the HE_{11} mode in large core waveguides approaches the TE or TM mode.

Fig. 10(a) and (b) show the resultant boundary which is determined whether the absolute value of P is greater (TE mode) or less (TM mode) than unity at the core diameter of 0.1 mm. In the region where n is smaller than unity, i.e., in total reflection-type waveguides, the HE_{11} mode tends to approach the TM mode. However, when n is larger than unity, the HE_{11} mode tends to approach the TE mode or to the TM mode as shown in Fig. 10(a) and (b) depending on κ.

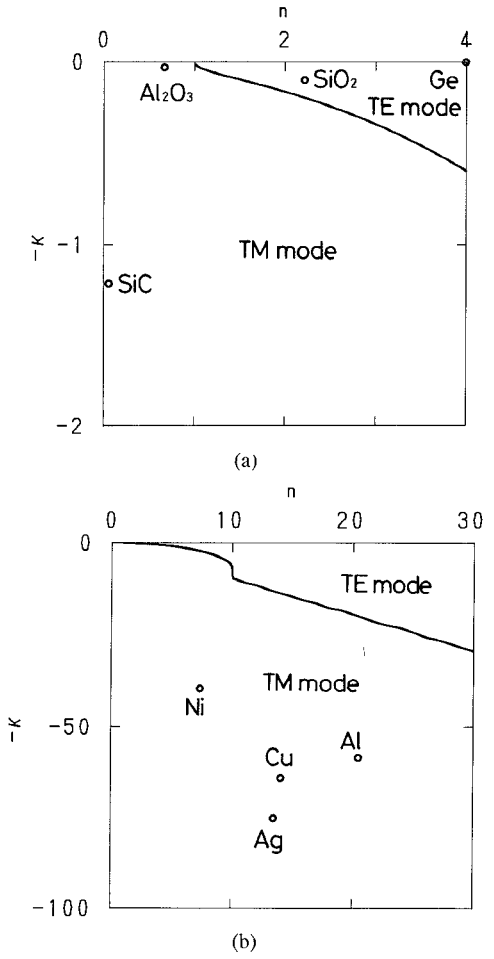

Fig. 10. Boundary curve dividing the TE and TM modes in a small core waveguide corresponding to the HE_{11} mode in the plane of complex refractive index of cladding materials [5], [17], [22]. (a) $n \leqq 4$. (b) $n \leqq 30$.

One may realize that the kink point of the boundary line exists at $n = 10$. In the region where n is not large, the change of $|P|$ value is small around the boundary line like a SiO_2 hollow waveguide. When κ is sufficiently large, the change of $|P|$ value is drastic as is seen in the metallic waveguide. Therefore, there is a possibility of a kink point in the boundary line, which is only proved by numerical calculations.

VI. Conclusion

We have numerically solved the exact characteristic equations of the hollow waveguides consisting of a single cladding material with various complex refractive indices. It has been made clear that the mode properties change drastically as the core diameter becomes small which depend on cladding materials and mode orders. In metallic hollow waveguides, it has been found that the HE_{11}, EH_{11}, and TM_{01} modes in large core waveguides approach the TM_{11}, TE_{12}, and TM_{02} modes in small core waveguides. Special modes are also analyzed in metallic waveguides which smoothly approach familiar modes in perfect-conducting circular waveguides when the core diameters become small. In dielectric hollow waveguides with relatively small κ, the HE_{11} mode tends to approach the TE or TM mode depending on cladding materials. Furthermore, we have pointed out that there are some regions of the core diameters whose attenuation constants in metallic hollow waveguides cannot be evaluated by using the previous approximate formulas.

References

[1] E Garmire, T. McMahon, and M. Bass, "Flexible infrared waveguides for high-power transmission," *IEEE J. Quantum Electron.*, vol. QE-16, pp 23-32, Jan. 1980

[2] M. E. Marhic, L. I. Kwan, and M. Epstein, "Invariant properties of helical-circular metallic waveguides," *Appl. Phys. Lett.*, vol. 33, no. 10, pp. 874-876, Nov. 1978.

[3] R. M. Jenkins and R. W. J. Devereux, "Transmission characteristics of a curved hollow silica waveguide at 10.6 μm," *IEEE J. Quantum Electron.*, vol. QE-22, pp. 718-722, May 1986.

[4] T. Hidaka, K. Kumada, J. Shimada, and T. Morikawa, "GeO_2-ZnO-K_2O glass as the cladding material of 940-cm^{-1} CO_2 laser-light transmitting hollow-core waveguides," *J. Appl. Phys.*, vol 53, no. 8, pp. 5484-5940, Aug. 1982.

[5] J. A. Harrington and C C. Gregory, "Hollow sapphire fibers for the delivery of CO_2 laser energy," *Opt. Lett.*, vol. 15, no. 10, pp. 541-543, May 1990.

[6] M. Miyagi and S. Kawakami, "Design theory of dielectric-coated circular metallic waveguides for infrared transmission," *IEEE J. Lightwave Technol.*, vol. LT-2, pp. 116-126, Apr. 1984.

[7] A. Hongo, K. Morosawa, T. Siota, Y. Matsuura, and M. Miyagi, "Transmission characteristics of germanium thin-film-coated metallic hollow waveguides for high-powered CO_2 laser light," *IEEE J. Quantum Electron.*, vol. 26, pp. 1510-1515, Sept. 1990.

[8] A. Hongo, K. Morosawa, T. Siota, K. Suzuki, S. Iwasaki, and M. Miyagi, "Transmission of 1 kW-class CO_2 laser light through circular hollow waveguides for material processing," *Appl. Phys. Lett.*, vol. 58, no. 15, pp. 1582-1584, Apr. 1991.

[9] Y. Kato, Y. Matsuura, T. Nakamura, and M. Miyagi, "A novel fabrication method of dielectric-coated metallic hollow waveguides by all electroplating," *Trans. Inst. Electron. Inform. Commun. Eng.*, vol. J73-C-1, no. 6, pp. 481-483, June 1990, in Japanese.

[10] E. A. J. Marcatili and R A. Schmeltzer, "Hollow metallic and dielectric waveguides for long distance optical transmission and lasers," *Bell Syst. Tech. J.*, vol. 43, pp. 1783-1809, July 1964.

[11] M. Miyagi, *Hikari Denso No Kiso (Introduction to Optical Fiber Transmission).* Shokodo: Tokyo, Japan; 1991, pp. 128-135, in Japanese.

[12] E. Snitzer, "Cylindrical dielectric waveguide modes," *J. Opt. Soc. Amer.*, vol. 51, no. 5, pp. 491-498, May 1961.

[13] A. Safaai-Jazi and G. L. Yip, "Classification of hybrid modes in cylindrical dielectric optical waveguides," *Radio Sci.*, vol. 12, no. 4, pp. 603-609, July-Aug. 1977.

[14] K. Morishita, "Hybrid modes in circular cylindrical optical fibers," *IEEE Trans. Microwave Theory Tech.*, vol. MTT-31, pp. 344-350, Apr. 1983.

[15] H. Nagashima, *Suchi Keisan Ho (Method of Numerical Computations).* Maki Shoten: Tokyo, Japan, 1979, pp. 164-165, in Japanese.

[16] M. Abramowitz and I. A. Stegun, *Handbook of Mathematical Functions.* New York: Dover, 1972, p. 364.

[17] E. D. Palik, *Handbook of Optical Constants of Solids*, pt II, Orlando, FL: Academic Press, 1985, pp. 280-764.

[18] C. D. W. Wilkinson, "Application of electron beam lithography to integrated optics," *Proc. Third European Conf. ECIO'85*, pp. 30-33, 1985.

[19] M. Gastine, L. Courtois, and J. L. Dormann, "Electromagnetic resonances of free dielectric spheres," *IEEE Trans. Microwave Theory Tech.*, vol. MTT-15, pp. 694-700, Dec. 1967.

[20] J. J. Burke, G. I. Stegeman, and T. Tamir, "Surface-polariton-like waves guided by thin, lossy metal films," *Phys. Rev. B*, vol. 33, no. 8, pp. 5186-5201, Apr. 1986.

[21] K. Thyagarajan, S. Diggavi, A. K. Ghatak, W. Johnstone, G. Stewart, and B. Culshaw, "Thin-metal-clad waveguide polarizers anal-

ysis and comparison with experiment," *Opt. Lett.*, vol. 15, no. 18, pp. 1041–1043, Sept. 1990.

[22] K. Kudo, *Kiso Bussei Zuhyo (Table of Fundamental Properties of Materials)*. Kyoritsu Shuppan: Tokyo, Japan, 1972, pp. 128–133, in Japanese.

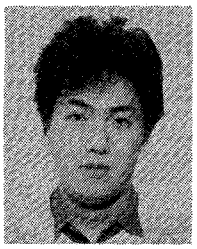

Yuji Kato was born in Sapporo, Japan, on June 9, 1966. He received the B.E. and M.E. degrees from Tohoku University, Sendai, Japan, in 1989 and 1991, respectively.

He is currently working towards the Ph.D. degree in electrical engineering at the Tohoku University. His research interests include hollow waveguides transmitting laser light in the mid-IR region.

Mr. Kato is a member of the Institute of Electronics and Communication Engineers of Japan.

Mitsunobu Miyagi (M'85–SM'90) was born in Hokkaido, Japan, on December 12, 1942. He graduated from Tohoku University, Sendai, Japan in 1965, and received the M.E. and Ph.D. degrees from the same university in 1967 and 1970, respectively.

He was appointed Research Associate at the Research Institute of Electrical Communication, Tohoku University, in 1970. From 1975 to 1977, on leave of absence of Tohoku University, he joined McGill University, Montreal, PQ, Canada, where he was engaged in research on optical communications. In 1978, he became an Associate Professor at the Research Institute of Electrical Communication. Since 1987, he has been a Professor at the Department of Electrical Communications, Faculty of Engineering, Tohoku University. He spent a month at Tianjin University, China, as a Consultant to the International Advisory Panel of the Chinese University Development Project and the Chinese Review Commission of the Chinese Ministry of Education in 1985. His research activities cover fiber optics, integrated optics, and guided wave technology and its application at mid-infrared, especially the design and fabrication of IR waveguides for high-powered CO_2 lasers and waveguide-type lasers. He also has been carrying out some works in electromagnetic theory including nonlinear wave propagation.

Dr. Miyagi is a member of the Institute of Electronics and Communication Engineers of Japan, the Optical Society of America, SPIE, and the American Institute of Physics. In 1989, he was awarded the Ichimura Prize for his contribution to the IR hollow waveguide and its application.